

Revisiting the Optical Signatures of BODIPY with *Ab Initio* Tools: Electronic Supplementary Information

Siwar Chibani^a, Boris Le Guennic^{*b}, Azzam Charaf-Eddin^a, Adèle D. Laurent^a and Denis Jacquemin^{*a,c}

Received Xth XXXXXXXXXX 20XX, Accepted Xth XXXXXXXXXX 20XX

First published on the web Xth XXXXXXXXXX 200X

DOI: 10.1039/b000000x

S1 Detailed computational protocol for AFCP

The estimation of the 0-0 energies follows a series of computational steps, systematically using the 6-31G(d) basis set except when noted:

1. Optimize the ground-state geometry (R^{GS}). This yields the total ground-state energy, $E^{\text{GS}}(R^{\text{GS}}, \text{eq})$, that is computed with both the 6-31G(d) and 6-311+G(2d,p) atomic basis set.
2. Compute the zero-point vibrational energy (ZPVE) of the GS, $E^{\text{ZPVE}}(R^{\text{GS}}, \text{eq})$.
3. Obtain vertical absorption energies within both the equilibrium and non-equilibrium limits using the SS approach:

$$E^{\text{abso}}(\text{SS}, \text{neq}) = E^{\text{ES}}(R^{\text{GS}}, \text{SS}, \text{neq}) - E^{\text{GS}}(R^{\text{GS}}, \text{eq}), \quad (\text{S-1})$$

$$E^{\text{abso}}(\text{SS}, \text{eq}) = E^{\text{ES}}(R^{\text{GS}}, \text{SS}, \text{eq}) - E^{\text{GS}}(R^{\text{GS}}, \text{eq}), \quad (\text{S-2})$$

$$\Delta E_{\text{neq/eq}}^{\text{abso}}(\text{SS}) = E^{\text{abso}}(\text{SS}, \text{neq}) - E^{\text{abso}}(\text{SS}, \text{eq}). \quad (\text{S-3})$$

4. Optimize the excited-state geometry (R^{ES}) with TD-DFT using the LR-PCM model. This step is performed within the equilibrium limit and therefore provides the excited-state energy of the relaxed ES, $E^{\text{ES}}(R^{\text{ES}}, \text{LR}, \text{eq})$, and allows to determine the adiabatic energy at the LR-PCM level,

$$E^{\text{adia}}(\text{LR}, \text{eq}) = E^{\text{ES}}(R^{\text{ES}}, \text{LR}, \text{eq}) - E^{\text{GS}}(R^{\text{GS}}, \text{eq}), \quad (\text{S-4})$$

where the GS energy calculated in Step 1 is used on the right-hand side.

5. Obtain the 6-311+G(2d,p) $E^{\text{ES}}(R^{\text{ES}}, \text{LR}, \text{eq})$ through a single point TD-DFT calculation performed on the 6-31G(d) ES geometry. Determine the 6-311+G(2d,p) $E^{\text{adia}}(\text{LR}, \text{eq})$ through Eq. (S-4) and calculate the amplitude of basis set effects,

$$\Delta E_{\text{BS-corr}}^{\text{adia}}(\text{LR}, \text{eq}) = E_{6-311+G(2d,p)}^{\text{adia}}(\text{LR}, \text{eq}) - E_{6-31G(d)}^{\text{adia}}(\text{LR}, \text{eq}) \quad (\text{S-5})$$

6. Determine the energy of the ES at its optimal geometry using the SS model in order to obtain SS adiabatic energies,

$$E^{\text{adia}}(\text{SS}, \text{eq}) = E^{\text{ES}}(R^{\text{ES}}, \text{SS}, \text{eq}) - E^{\text{GS}}(R^{\text{GS}}, \text{eq}) \quad (\text{S-6})$$

7. Compute the ZPVE of the excited-state, $E^{\text{ZPVE}}(R^{\text{ES}}, \text{LR}, \text{eq})$, and next the variation of the ZPVE between the two states,

$$\Delta E^{\text{ZPVE}}(\text{LR}, \text{eq}) = E^{\text{ZPVE}}(R^{\text{ES}}, \text{LR}, \text{eq}) - E^{\text{ZPVE}}(R^{\text{GS}}, \text{eq}), \quad (\text{S-7})$$

using the results of Step 2. $\Delta E^{\text{ZPVE}}(\text{LR}, \text{eq})$ is systematically negative in the present work, an expected trend for organic dyes. Indeed, the potential energy surfaces of the ES tend to be flatter than their GS counterpart, and consequently the ZPVE effects are smaller for the former.

8. Determine basis set corrected 0-0 energies by adding the results of Steps 5, 6 and 7:

$$E^{0-0}(\text{SS}, \text{eq}) = E^{\text{adia}}(\text{SS}, \text{eq}) + \Delta E_{\text{BS-corr}}^{\text{adia}}(\text{LR}, \text{eq}) + \Delta E^{\text{ZPVE}}(\text{LR}, \text{eq}). \quad (\text{S-8})$$

^a CEISAM, UMR CNRS 6230, BP 92208, Université de Nantes, 2, Rue de la Houssinière, 44322 Nantes, Cedex 3, France. Tel: +33-2-51-12-55-64; E-mail: Denis.Jacquemin@univ-nantes.fr

^b Institut des Sciences Chimiques de Rennes, Université de Rennes 1, CNRS 6226, 35042 Rennes Cedex, France.

^c Institut Universitaire de France, 103, bd Saint-Michel, F-75005 Paris Cedex 05, France.

9. Similarly to Step 3, obtain the SS fluorescence energies within both PCM limits,

$$E^{\text{fluo}}(\text{SS, neq}) = E^{\text{ES}}(R^{\text{ES}}, \text{SS, eq}) - E^{\text{GS}}(R^{\text{ES}}, \text{neq}), \quad (\text{S-9})$$

$$E^{\text{fluo}}(\text{SS, eq}) = E^{\text{ES}}(R^{\text{ES}}, \text{SS, eq}) - E^{\text{GS}}(R^{\text{ES}}, \text{eq}). \quad (\text{S-10})$$

$$\Delta E_{\text{neq/eq}}^{\text{fluo}}(\text{SS}) = E^{\text{fluo}}(\text{SS, neq}) - E^{\text{fluo}}(\text{SS, eq}). \quad (\text{S-11})$$

10. Correct the 0-0 energies of Step 8 for non-equilibrium effects, so to mimic the AFCP,

$$E^{\text{AFCP}}(\text{SS, neq}) = E^{0-0}(\text{SS, eq}) + \Delta E_{\text{neq/eq}}(\text{SS}) \quad (\text{S-12})$$

where $E^{0-0}(\text{SS, eq})$ comes from Step 8, whereas the correcting term has been determined from the data of Steps 3 and 9,

$$\Delta E_{\text{neq/eq}}(\text{SS}) = \frac{1}{2} \left(\Delta E_{\text{neq/eq}}^{\text{abso}}(\text{SS}) + \Delta E_{\text{neq/eq}}^{\text{fluo}}(\text{SS}) \right). \quad (\text{S-13})$$

The interested reader will find more details and justifications regarding this protocol in our two previous methodological contributions,^{1,2} but we underline that the $E^{\text{AFCP}}(\text{SS, neq})$ obtained in this way correspond to state-of-the-art estimates.

S2 Experimental and theoretical data for the test and training sets.

Table S-I Experimental wavelengths of absorption and fluorescence for the series of dyes of Figure 2 (in main text). All values are in nm.

Dye	Solvent	λ_{abso}	λ_{fluo}	Ref.
I	Cyclohexane	504	515	3
II	Ethyl Acetate	406	444	4
III	Cyclohexane	526	532	5
IV	Methanol	493	533	6,7
V	Dichloromethane	516	570	8
VI	Dichloromethane	527	587	8
VII	Dichloromethane	519	542	9
VIII	Toluene	555	578	10
IX	Methanol	564	593	11
X	Dichloromethane	641	643	12
XI	Dichloromethane	542	562	13
XII	Dichloromethane	612	629	13
XIII	Chloroform	579	583	14
XIV	Dichloromethane	415	430	15
XV	Dichloromethane	454	464	15
XVI	<i>n</i> -Hexane	450	456	16
XVII	Toluene	646	666	10
XVIII	Dichloromethane	711	733	17
XIX	Dichloromethane	403	480	18
XX	Dichloromethane	466	604	18
XXI	Dichloromethane	427	520	18
XXII	Dichloromethane	474	583	18
XXIII	Chloroform	758	774	19
XXIV	Chloroform	692	703	19

Table S-II E^{AFPC} determined with six different hybrid functionals (see protocol above). All values are in eV. Experimental values in Table S-I.

Dye	B3LYP	PBE0	BMK	M06-2X	CAM-B3LYP	ω B97X-D
I	2.859	2.947	2.988	2.947	2.975	2.984
II	3.209	3.312	2.889	3.375	3.406	3.431
III	2.692	2.739	2.757	2.729	2.755	2.741
IV	2.651	2.793	2.906	2.890	2.907	2.906
V	2.764	2.816	2.852	2.830	2.862	2.869
VI	2.405	2.454	2.532	2.499	2.543	2.566
VII	2.679	2.769	2.877	2.818	2.842	2.861
VIII	2.287	2.361	2.419	2.514	2.539	2.557
IX	2.299	2.350	2.403	2.451	2.470	2.528
X	2.068	2.114	2.209	2.197	2.201	2.234
XI	2.553	2.625	2.683	2.685	2.689	2.697
XII	2.198	2.252	2.337	2.319	2.322	2.267
XIII	2.544	2.585	2.604	2.568	2.575	2.574
XIV	3.053	3.147	3.293	3.336	3.323	3.330
XV	2.844	2.929	3.085	3.107	3.120	3.139
XVI	2.671	2.809	3.070	3.171	3.214	3.249
XVII	2.100	2.145	2.207	2.209	2.233	2.242
XVIII	1.888	1.937	1.994	2.015	2.011	2.027
XIX	2.659	2.819	3.128	3.191	3.145	3.172
XX	1.669	1.845	2.498	2.798	2.875	2.871
XXI	2.458	2.588	2.883	2.953	2.913	2.947
XXII	1.825	2.075	2.631	2.785	2.758	2.801
XXIII	1.722	1.787	1.926	1.970	1.963	1.991
XXIV	1.988	2.054	2.164	2.168	2.194	2.223

Table S-III Comparison between experimental and theoretical AFPC energies for the test set represented in Figure 4 (main text). All values are in eV and have been obtained with the M06-2X functional.

Dye	Solvent	Theory	Experiment	Ref.
XXV	Toluene	2.689	2.263	20
XXVI	Cyclohexane	2.612	2.265	21
XXVII	Cyclohexane	2.425	2.050	21
XXVIII	Dichloromethane	2.556	2.214	22
XXIX	Dichloromethane	2.142	1.899	22
XXX	Dichloromethane	3.653	3.500	7
XXXI	Ethanol	3.712	3.233	7
XXXII	Toluene	2.661	2.295	23
XXXIII	Toluene	2.647	2.259	23
XXXIV	Dichloromethane	2.383	2.028	24
XXXV	Dichloromethane	2.065	1.791	24

S3 MD simulations.

S3.1 Method

MD simulations of a single BODIPY molecule in dichloromethane solution were performed with the NAMD program.²⁵ Parameters of the dichloromethane have been generated with ParamChem²⁶ and the CGen force field has been used²⁷ while the BODIPY parameters have been taken from Song et. al.²⁸. The BODIPY molecule has been preliminary optimized with the level of theory used in the present study: M06-2X/6-31G(d,p). Atomic charges have been then computed at the HF/6-31G(d) level of theory with the ChelpG electrostatic potential fitting procedure.²⁹

The single pre-optimized BODIPY molecule was placed in the center of a cubic simulation box of (50) dimension. After a minimization step, the solvent alone was relaxed while the BODIPY was kept frozen for 100 ps with a timestep of 1.0 fs in the NPT ensemble. Eventually two isobare and isothermal runs of 200 ps (timestep is 2.0 fs) at 298 K were performed. BODIPY coordinates were extracted each two picoseconds. Therefore a total of 170 snapshots with the chromophore coordinates were employed to perform PCM(CH₂Cl₂)/TD-M06-2X/6-31G(d) computations.

Each spectra have been then fitted with a Gaussian of HWHM of 0.04 eV and averaged in order to obtain the Figure S-1.

S3.2 Result

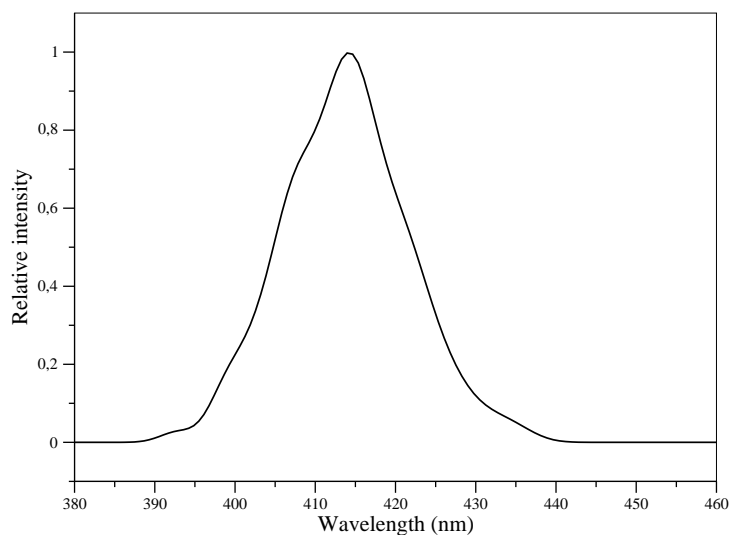


Fig. S-1 Averaged spectrum over 170 snapshots extracted from the MD simulation of bodipy chromogens into CH₂Cl₂ solvent.

S4 Additional simulation of spectral shapes.

S4.1 Absorption and emission of XVIII

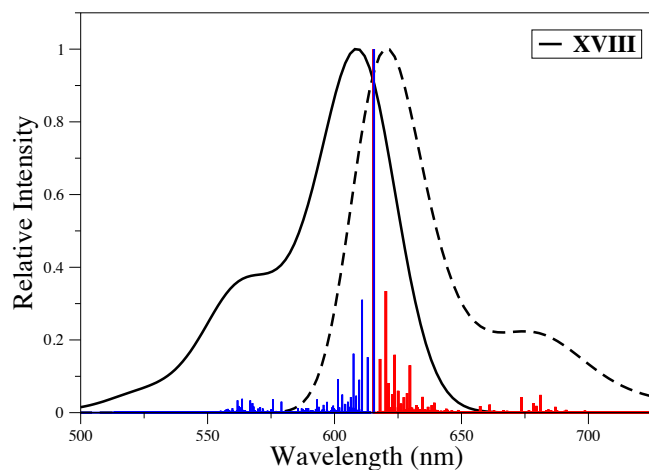


Fig. S-2 Absorption (full) and emission (dashed) spectra of XVIII. Experimental spectra might be found in Ref. 17.

S4.2 Emission of XIV and XV.

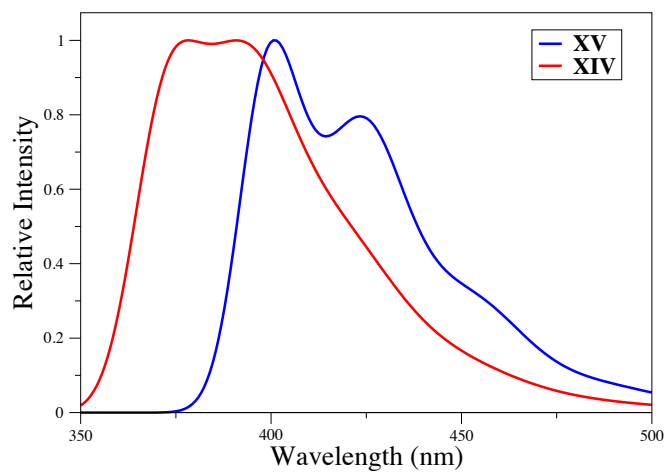


Fig. S-3 Emission spectra of XIV and XV. Experimental data can be found in Ref. 15

S4.3 Absorption and emission of XVI

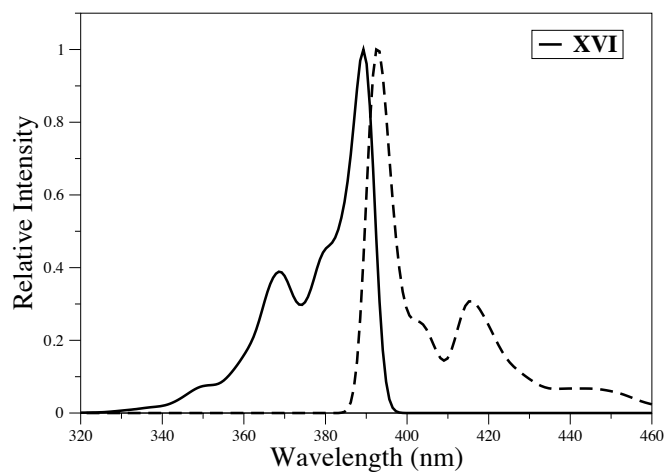


Fig. S-4 Absorption (full) and emission (dashed) spectra of XVI. Experimental spectra might be found in Ref. 16.

S4.4 Absorption and emission of XIX

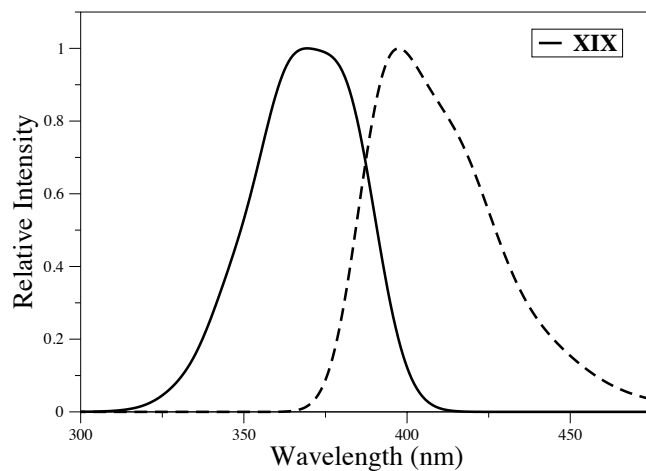


Fig. S-5 Absorption (full) and emission (dashed) spectra of XIX. Experimental spectra might be found in Ref. 18.

S4.5 Absorption and emission of XXXVI

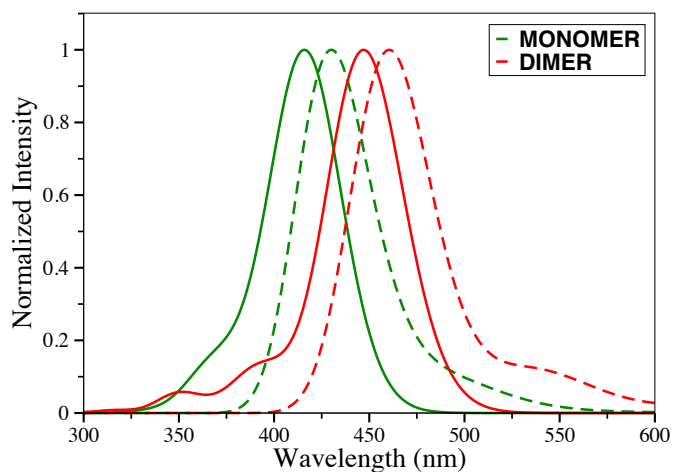


Fig. S-6 Absorption (full) and emission (dashed) spectra of **XXXVI** and the corresponding monomer. Experimental spectra can be found in Ref. ³⁰.

S4.6 Absorption and emission of XLI

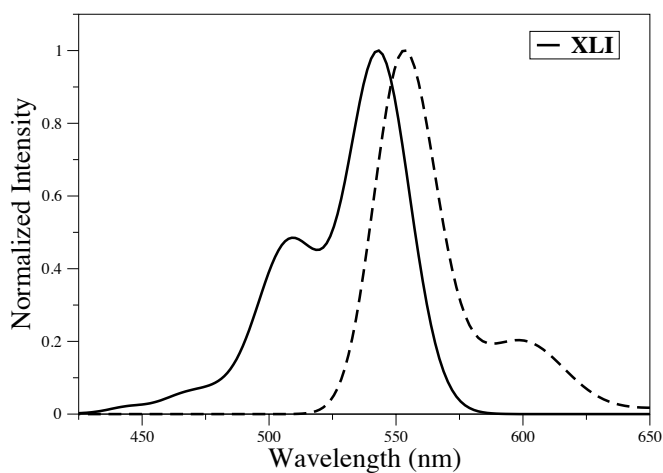


Fig. S-7 Absorption (full) and emission (dashed) spectra of **XLI**. Experimental spectra might be found in Ref. 31.

S4.7 Absorption and emission of XLII

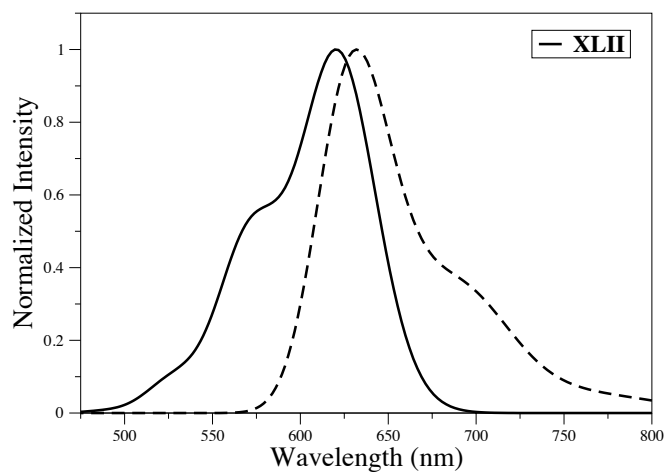


Fig. S-8 Absorption (full) and emission (dashed) spectra of **XLII**. Experimental spectra might be found in Ref. 31.

S5 Additional density difference plots.

S5.1 Density difference plots for XL

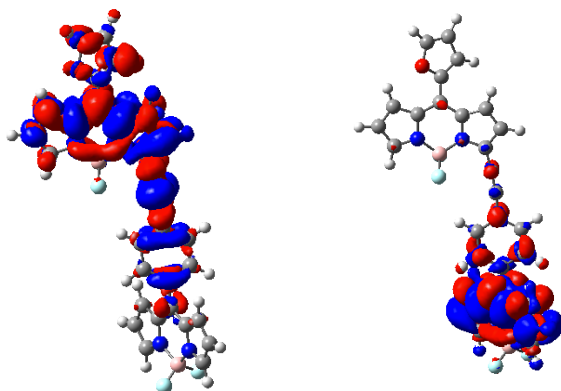


Fig. S-9 Density difference plots for the first (left) and second (right) ES of XL

S5.2 Density difference plots for XXXIX

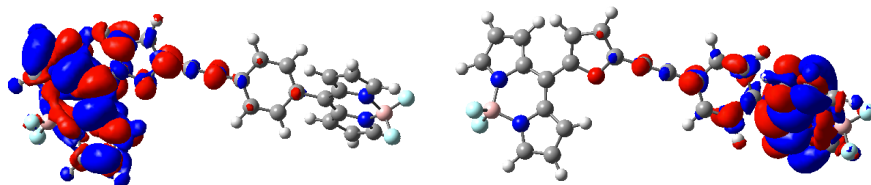


Fig. S-10 Density difference plots for the first (left) and second (right) ES of XXXIX

S5.3 Density difference plots for XLIII

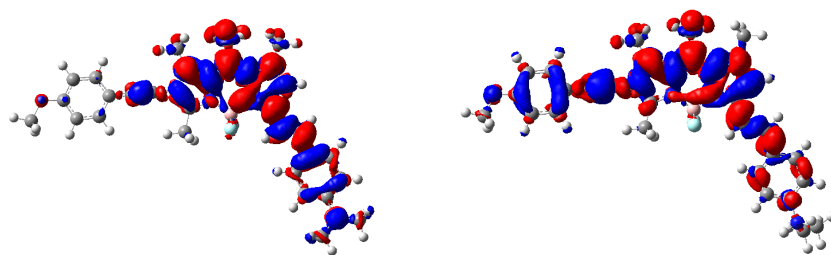


Fig. S-11 Density difference plots for the neutral (left) and protonated (right) ES of **XLIII**

S5.4 Density difference plots for two additional CT dyes

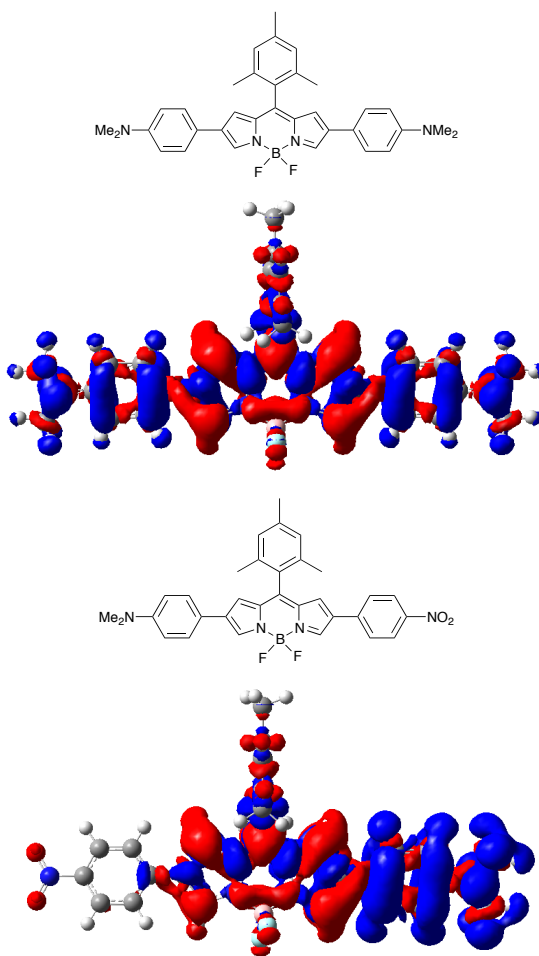


Fig. S-12 Density difference plots for two non-emissive dyes proposed by Hayashi and coworkers.³²

S6 Huang-Rhys factors.

S6.1 HR factors LXVI

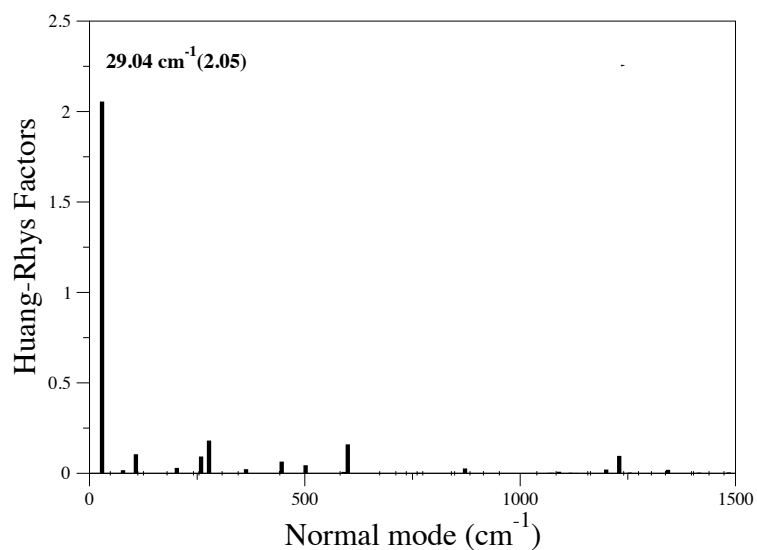


Fig. S-13 Computed HR factors for LXVI, the largest contributing mode is given.

S6.2 HR factors LXVII

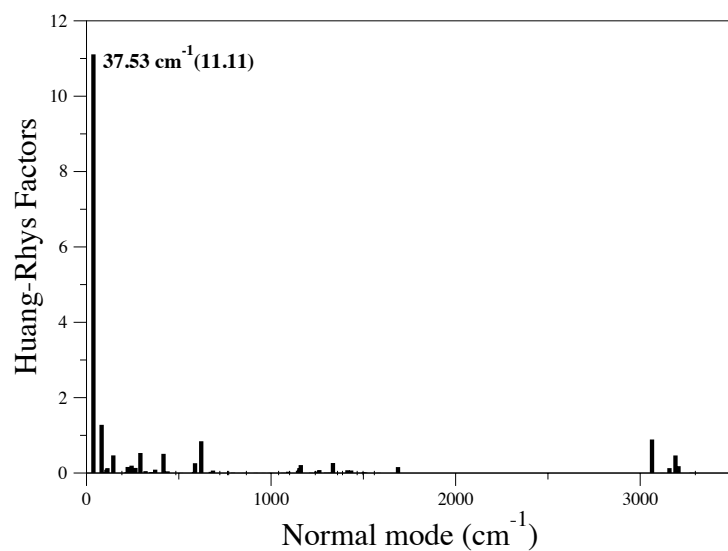


Fig. S-14 Computed HR factors for LXVII, the largest contributing mode is given.

S7 List of transition energies.

Table S-IV List of 6-31G(d) transition energies (eV) computed with TD-DFT. Note that values in the main text and in Section S2 for the AFCP energies are corrected for equilibrium/non-equilibrium difference, as well as for basis set effects. See Section S1 for more details.

BODIPY	Solvent	Functional	$E^{\text{abs}}(\text{SS}, \text{neq})$	$E^{\text{flu}}(\text{SS}, \text{neq})$	$E^{\text{adia}}(\text{SS}, \text{eq})$	$\Delta E^{\text{ZPVE}}(\text{LR}, \text{eq})$
I	Cyclohexane	B3LYP	3.170	2.899	3.044	-0.138
		PBE0	3.230	3.003	3.124	-0.120
		BMK	3.225	3.058	3.147	-0.107
		M06-2X	3.182	3.027	3.110	-0.091
		CAM-B3LYP	3.205	3.063	3.137	-0.090
		ω B97X-D	3.206	3.070	3.140	-0.083
II	EthylEthanoate	B3LYP	3.540	3.206	3.380	-0.106
		PBE0	3.642	3.296	3.484	-0.102
		BMK	3.732	3.100	3.301	-0.092
		M06-2X	3.747	3.314	3.544	-0.090
		CAM-B3LYP	3.747	3.363	3.565	-0.084
		ω B97X-D	3.760	3.364	3.576	-0.077
III	Cyclohexane	B3LYP	2.923	2.813	2.872	-0.111
		PBE0	2.972	2.851	2.915	-0.105
		BMK	2.993	2.872	2.932	-0.123
		M06-2X	2.976	2.797	2.888	-0.093
		CAM-B3LYP	2.995	2.814	2.905	-0.083
		ω B97X-D	2.997	2.809	2.906	-0.103
IV	Methanol	B3LYP	2.942	2.738	2.836	-0.119
		PBE0	3.053	2.853	2.957	-0.111
		BMK	3.114	2.917	3.019	-0.061
		M06-2X	3.113	2.904	3.014	-0.080
		CAM-B3LYP	3.137	2.927	3.039	-0.087
		ω B97X-D	3.130	2.894	3.023	-0.080
V	Dichloromethane	B3LYP	2.994	2.858	2.921	-0.089
		PBE0	3.039	2.908	2.968	-0.083
		BMK	3.070	2.949	3.005	-0.085
		M06-2X	3.029	2.918	2.969	-0.061
		CAM-B3LYP	3.058	2.951	3.000	-0.063
		ω B97X-D	3.068	2.962	3.012	-0.063
VI	Dichloromethane	B3LYP	2.611	2.430	2.525	-0.070
		PBE0	2.667	2.488	2.582	-0.070
		BMK	2.733	2.532	2.635	-0.051
		M06-2X	2.742	2.541	2.630	-0.060
		CAM-B3LYP	2.775	2.568	2.676	-0.057
		ω B97X-D	2.798	2.582	2.696	-0.054

Table S-V List of transition energies computed with TD-DFT. See caption of Table S-IV for more details.

BODIPY	Solvent	Functional	$E^{\text{abs}}(\text{SS, neq})$	$E^{\text{flu}}(\text{SS, neq})$	$E^{\text{adia}}(\text{SS, eq})$	$\Delta E^{\text{ZPVE}}(\text{LR, eq})$
VII	Dichloromethane	B3LYP	2.939	2.717	2.811	-0.092
		PBE0	3.012	2.818	2.907	-0.088
		BMK	3.062	2.876	2.963	-0.051
		M06-2X	3.052	2.882	2.954	-0.072
		CAM-B3LYP	3.065	2.886	2.964	-0.067
		ω B97X-D	3.082	2.909	2.983	-0.058
VIII	Toluene	B3LYP	2.585	2.215	2.416	-0.093
		PBE0	2.683	2.293	2.499	-0.089
		BMK	2.739	2.389	2.590	-0.148
		M06-2X	2.743	2.474	2.636	-0.066
		CAM-B3LYP	2.774	2.485	2.661	-0.076
		ω B97X-D	2.780	2.533	2.683	-0.075
IX	Methanol	B3LYP	2.494	2.281	2.390	-0.066
		PBE0	2.550	2.338	2.447	-0.065
		BMK	2.618	2.391	2.510	-0.093
		M06-2X	2.635	2.416	2.526	-0.036
		CAM-B3LYP	2.661	2.423	2.546	-0.045
		ω B97X-D	2.710	2.445	2.572	-0.017
X	Dichloromethane	B3LYP	2.247	2.083	2.167	-0.058
		PBE0	2.297	2.130	2.215	-0.058
		BMK	2.345	2.168	2.260	-0.018
		M06-2X	2.361	2.185	2.276	-0.031
		CAM-B3LYP	2.374	2.181	2.284	-0.041
		ω B97X-D	2.389	2.197	2.301	-0.024
XI	Dichloromethane	B3LYP	2.787	2.661	2.721	-0.088
		PBE0	2.849	2.722	2.783	-0.083
		BMK	2.895	2.749	2.821	-0.076
		M06-2X	2.908	2.740	2.821	-0.067
		CAM-B3LYP	2.913	2.742	2.826	-0.066
		ω B97X-D	2.914	2.740	2.826	-0.063
XII	Dichloromethane	B3LYP	2.381	2.262	2.325	-0.072
		PBE0	2.434	2.312	2.378	-0.070
		BMK	2.494	2.356	2.431	-0.050
		M06-2X	2.509	2.368	2.443	-0.063
		CAM-B3LYP	2.512	2.356	2.440	-0.058
		ω B97X-D	2.621	2.358	2.386	-0.069
XIII	Chloroform	B3LYP	2.744	2.678	2.716	-0.108
		PBE0	2.782	2.713	2.752	-0.103
		BMK	2.783	2.703	2.748	-0.095
		M06-2X	2.754	2.675	2.718	-0.086
		CAM-B3LYP	2.761	2.678	2.725	-0.083
		ω B97X-D	2.756	2.669	2.718	-0.076
XIV	Dichloromethane	B3LYP	3.396	3.018	3.209	-0.097
		PBE0	3.492	3.099	3.295	-0.093
		BMK	3.672	3.203	3.430	-0.085
		M06-2X	3.728	3.223	3.466	-0.081
		CAM-B3LYP	3.721	3.227	3.464	-0.081
		ω B97X-D	3.724	3.235	3.467	-0.085

Table S-VI List of transition energies computed with TD-DFT. See caption of Table S-IV for more details.

BODIPY	Solvent	Functional	$E^{\text{abs}}(\text{SS, neq})$	$E^{\text{flu}}(\text{SS, neq})$	$E^{\text{adia}}(\text{SS, eq})$	$\Delta E^{\text{ZPVE}}(\text{LR, eq})$
XV	Dichloromethane	B3LYP	3.110	2.827	2.972	-0.092
		PBE0	3.198	2.904	3.054	-0.089
		BMK	3.369	3.011	3.190	-0.078
		M06-2X	3.426	3.032	3.225	-0.080
		CAM-B3LYP	3.431	3.050	3.236	-0.075
		ω B97X-D	3.437	3.060	3.243	-0.069
XVI	<i>n</i> -hexane	B3LYP	3.250	2.415	2.820	-0.103
		PBE0	3.358	2.597	2.967	-0.105
		BMK	3.515	2.961	3.245	-0.119
		M06-2X	3.535	3.252	3.394	-0.142
		CAM-B3LYP	3.558	3.349	3.452	-0.153
		ω B97X-D	3.569	3.365	3.466	-0.139
XVII	Toluene	B3LYP	2.275	2.149	2.218	-0.079
		PBE0	2.325	2.199	2.267	-0.078
		BMK	2.372	2.237	2.310	-0.076
		M06-2X	2.388	2.258	2.329	-0.066
		CAM-B3LYP	2.406	2.268	2.343	-0.063
		ω B97X-D	2.418	2.277	2.354	-0.065
XVIII	Dichloromethane	B3LYP	2.052	1.933	1.994	-0.071
		PBE0	2.102	1.975	2.040	-0.069
		BMK	2.168	2.019	2.096	-0.074
		M06-2X	2.187	2.023	2.107	-0.053
		CAM-B3LYP	2.182	2.010	2.099	-0.052
		ω B97X-D	2.190	2.008	2.103	-0.042
XIX	Dichloromethane	B3LYP	3.164	2.469	2.752	-0.089
		PBE0	3.293	2.669	2.926	-0.090
		BMK	3.528	3.004	3.239	-0.079
		M06-2X	3.611	3.070	3.321	-0.085
		CAM-B3LYP	3.560	3.049	3.283	-0.083
		ω B97X-D	3.575	3.051	3.291	-0.073
XX	Dichloromethane	B3LYP	2.238	1.294	1.668	-0.065
		PBE0	2.409	1.489	1.835	-0.069
		BMK	2.856	2.257	2.499	-0.076
		M06-2X	3.041	2.609	2.824	-0.064
		CAM-B3LYP	3.083	2.685	2.892	-0.060
		ω B97X-D	3.186	2.731	2.940	-0.057
XXI	Dichloromethane	B3LYP	2.997	2.228	2.572	-0.100
		PBE0	3.111	2.368	2.708	-0.100
		BMK	3.324	2.759	3.018	-0.113
		M06-2X	3.407	2.750	3.068	-0.080
		CAM-B3LYP	3.365	2.762	3.041	-0.085
		ω B97X-D	3.378	2.778	3.055	-0.080
XXII	Dichloromethane	B3LYP	2.348	1.470	1.801	-0.072
		PBE0	2.523	1.747	2.043	-0.072
		BMK	2.909	2.424	2.646	-0.074
		M06-2X	3.058	2.595	2.820	-0.041
		CAM-B3LYP	3.079	2.615	2.834	-0.065
		ω B97X-D	3.148	2.646	2.872	-0.050

Table S-VII List of transition energies computed with TD-DFT. Only the lowest-lying excited-state reported. nc indicates that the excited-state calculation failed to converge to a meaningful states. See caption of Table S-IV for more details.

BODIPY	Form	Solvent	Functional	$E^{\text{abs}}(\text{SS, neq})$	$E^{\text{fluo}}(\text{SS, neq})$	$E^{\text{adia}}(\text{SS, eq})$	$\Delta E^{\text{ZPVE}}(\text{LR, eq})$
XXIII		Chloroform	B3LYP	1.888	1.792	1.842	-0.073
			PBE0	1.959	1.851	1.906	-0.072
			BMK	2.096	1.953	2.028	-0.056
			M06-2X	2.159	1.979	2.069	-0.052
			CAM-B3LYP	2.160	1.972	2.068	-0.054
			ω B97X-D	2.204	2.008	2.109	-0.069
XXIV		Chloroform	B3LYP	2.152	2.096	2.126	-0.094
			PBE0	2.211	2.151	2.183	-0.085
			BMK	2.307	2.228	2.269	-0.067
			M06-2X	2.332	2.232	2.284	-0.069
			CAM-B3LYP	2.350	2.245	2.298	-0.058
			ω B97X-D	2.382	2.275	2.329	-0.061
XXV		Toluene	B3LYP	2.896	2.155	2.607	-0.110
			PBE0	2.970	2.257	2.699	-0.104
			BMK	3.009	2.530	2.818	-0.089
			M06-2X	3.001	2.514	2.822	-0.092
			CAM-B3LYP	3.026	2.600	2.859	-0.082
			ω B97X-D	3.044	2.599	2.879	-0.082
XXVI		Cyclohexane	B3LYP	2.676	nc	nc	nc
			PBE0	2.743	2.243	2.472	-0.074
			BMK	2.844	2.524	2.673	-0.068
			M06-2X	2.878	2.604	2.734	-0.080
			CAM-B3LYP	2.908	2.631	2.760	-0.059
			ω B97X-D	2.931	2.667	2.789	-0.052
XXVII		Cyclohexane	B3LYP	2.424	2.231	2.321	-0.079
			PBE0	2.479	2.303	2.384	-0.070
			BMK	2.545	2.397	2.470	-0.066
			M06-2X	2.562	2.436	2.499	-0.047
			CAM-B3LYP	2.599	2.471	2.534	-0.046
			ω B97X-D	2.615	2.492	2.552	-0.023
XXVIII		Dichloromethane	M06-2X	2.792	2.642	2.710	-0.084
XXIX		Dichloromethane	M06-2X	2.371	2.206	2.282	-0.069
XXX		Dichloromethane	M06-2X	4.349	3.495	3.902	-0.125
XXXI		Ethanol	M06-2X	4.242	3.421	3.820	-0.112
XXXII		Toluene	M06-2X	2.867	2.606	2.735	-0.064
XXXIII		Toluene	M06-2X	2.806	2.649	2.733	-0.058
XXXIV		Dichloromethane	M06-2X	2.598	2.416	2.515	-0.063
XXXV		Dichloromethane	M06-2X	2.279	2.060	2.175	-0.056
XXXVI	Monomer	Dichloromethane	M06-2X	3.099	2.959	3.037	-0.068
	Dimer		M06-2X	2.893	2.754	2.826	-0.085
XXXVII	Monomer	Dichloromethane	M06-2X	3.146	3.013	3.077	-0.072
	Dimer		M06-2X	2.709	2.488	2.603	-0.062
XXXVIII	Monomer	Toluene	M06-2X	2.485	2.283	2.382	-0.084
	Dimer		M06-2X	2.170	1.803	1.996	-0.095
XXXIX		Toluene	M06-2X	2.963	2.424	2.749	-0.077
XL		Toluene	M06-2X	2.637	2.387	2.525	-0.066

Table S-VIII List of transition energies computed with TD-DFT. All calculations with M06-2X. Only the lowest-lying excited-state reported except when noted. See caption of Table S-IV for more details.

BODIPY	Form	Solvent	$E^{\text{abs}}(\text{SS, neq})$	$E^{\text{flu}}(\text{SS, neq})$	$E^{\text{adia}}(\text{SS, eq})$	$\Delta E^{\text{ZPVE}}(\text{LR, eq})$
XLI	Neutral	Chloroform	2.457	2.275	2.372	-0.065
	Diprotonated		2.414	2.154	2.286	-0.081
XLII	Neutral	Chloroform	2.159	1.930	2.051	-0.046
	Diprotonated		2.476	2.260	2.372	-0.047
XLIII	Neutral	Dioxan	2.438	2.245	2.348	-0.080
	Protonated		2.567	2.237	2.398	-0.082
XLIV	Neutral	Water	2.682	2.460	2.579	-0.063
	Protonated		2.737	2.571	2.681	-0.063
	Deprotonated		2.615	2.352	2.475	-0.041
XLV	Neutral	Tetrahydrofuran	2.458	2.199	2.343	-0.038
	Protonated		2.744	2.559	2.672	-0.068
	Deprotonated (S1)		2.461	0.282	0.922	-0.060
	Deprotonated (S2)		2.461	2.216	2.487	-0.088
XLVI		Acetonitrile	3.062	2.958	3.008	-0.091
XLVII	Free	Acetonitrile	2.682	2.460	2.588	-0.047
	With $\text{CN}^-/\text{NH}_4^+$		2.633	2.279	2.458	-0.046
XLVIII	C=S	Chloroform	2.822	2.538	2.667	-0.057
	C=O		2.935	2.754	2.839	-0.065
XLIX	Dithiane	Tetrahydrofuran	3.022	2.817	2.908	-0.074
	Carbonyl		3.128	2.922	3.013	-0.062
L	Sulfur	Dichloromethane	2.839	2.684	2.740	-0.057
	Sulfoxyde		3.078	2.812	2.933	-0.069
LI	wo biphenyl	Dichloromethane	3.146	3.013	3.077	-0.073
LI	w biphenyl	Dichloromethane	2.698	2.482	2.577	-0.051
LII		Dichloromethane	2.368	2.268	2.317	-0.054
LIII		Toluene	3.063	2.915	2.993	-0.082
LIV		Toluene	2.899	2.797	2.847	-0.087
LV		Toluene	2.843	2.684	2.765	-0.076
LVI		Toluene	2.519	2.398	2.461	-0.059
LVII		Chloroform	2.487	2.245	2.366	-0.044
LVIII		Chloroform	2.485	2.241	2.363	-0.041
LIX		Dichloromethane	3.064	2.887	2.969	-0.072
LX		Dichloromethane	2.967	2.753	2.844	-0.053
LXI		Dichloromethane	2.797	2.598	2.692	-0.053
LXII		Chloroform	2.604	2.504	2.560	-0.095
LXIII		Chloroform	2.431	2.310	2.379	-0.071
LXIV		Chloroform	2.340	2.208	2.280	-0.061
LXV		Chloroform	2.179	2.038	2.115	-0.057
LXVI		Tetrahydrofuran	3.197	3.054	3.127	-0.082
LXVII		Tetrahydrofuran	3.129	2.691	2.955	-0.065

References

- 1 D. Jacquemin, A. Planchat, C. Adamo and B. Mennucci, *J. Chem. Theory Comput.*, 2012, **8**, 2359–2372.
- 2 S. Chibani, B. Le Guennic, A. Charaf-Eddin, O. Maury, C. Andraud and D. Jacquemin, *J. Chem. Theory Comput.*, 2012, **8**, 3303–3313.
- 3 I. J. Arroyo, R. Hu, G. Merino, B. Z. Tang and E. Pena-Cabrera, *J. Org. Chem.*, 2009, **74**, 5719–5722.
- 4 J. Banuelos, V. Martin, C. F. A. Gomez-Duran, I. J. A. Cordoba, E. Pena-Cabrera, I. Garcia-Moreno, A. Costela, M. E. Perez-Ojeda, T. Arbeloa and I. L. Arbeloa, *Chem. Eur. J.*, 2011, **17**, 7261–7270.
- 5 M. Liras, J. Bañuelos Prieto, M. Pintado-Sierra, I. García-Moreno, Á. Costela, L. Infantes, R. Sastre and F. Amat-Guerri, *Org. Lett.*, 2007, **9**, 4183–4186.
- 6 T. G. Pavlopoulos, J. H. Boyer, M. Shah, K. Thangaraj and M. L. Soong, *Appl. Opt.*, 1990, **29**, 3885–3886.
- 7 A. Loudet and K. Burgess, *Chem. Rev.*, 2007, **107**, 4891–4932.
- 8 S. Rihn, P. Retailleau, N. Bugsaliewicz, A. D. Nicola and R. Ziessel, *Tetrahedron Lett.*, 2009, **50**, 7008 – 7013.
- 9 C. Yu, L. Jiao, H. Yin, J. Zhou, W. Pang, Y. Wu, Z. Wang, G. Yang and E. Hao, *Eur. J. Org. Chem.*, 2011, **2011**, 5460–5468.
- 10 V. Leen, D. Miscoria, S. Yin, A. Filarowski, J. Molisho Ngongo, M. Van der Auweraer, N. Boens and W. Dehaen, *J. Org. Chem.*, 2011, **76**, 8168–8176.
- 11 B. P. Wittmershaus, J. J. Skibicki, J. B. McLafferty, Y.-Z. Zhang and S. Swan, *J. Fluores.*, 2001, **11**, 119–128.
- 12 G. Ulrich, S. Goeb, A. De Nicola, P. Retailleau and R. Ziessel, *J. Org. Chem.*, 2011, **76**, 4489–4505.
- 13 L. Jiao, C. Yu, M. Liu, Y. Wu, K. Cong, T. Meng, Y. Wang and E. Hao, *J. Org. Chem.*, 2010, **75**, 6035–6038.
- 14 K. Umezawa, A. Matsui, Y. Nakamura, D. Citterio and K. Suzuki, *Chem. Eur. J.*, 2009, **15**, 1096–1106.
- 15 Y. Zhou, Y. Xiao, D. Li, M. Fu and X. Qian, *J. Org. Chem.*, 2008, **73**, 1571–1574.
- 16 Y. Kubota, T. Tsuzuki, K. Funabiki, M. Ebihara and M. Matsui, *Org. Lett.*, 2010, **12**, 4010–4013.
- 17 Y. Tomimori, T. Okujima, T. Yano, S. Mori, N. Ono, H. Yamada and H. Uno, *Tetrahedron*, 2011, **67**, 3187–3193.
- 18 Y. Kubota, H. Hara, S. Tanaka, K. Funabiki and M. Matsui, *Org. Lett.*, 2011, **13**, 6544–6547.
- 19 M. Nakamura, T. Tahara, K. Takahashi, T. Nagata, H. Uoyama, D. Kuzuhara, S. Mori, T. Okujima, H. Yamada and H. Uno, *Org. Biomol. Chem.*, 2012, **10**, 6840–6849.
- 20 T. K. Khan and M. Ravikanth, *Dyes Pigm.*, 2012, **95**, 89–95.
- 21 T. Rohand, M. Baruah, W. Qin, N. Boens and W. Dehaen, *Chem. Commun.*, 2006, 266–268.
- 22 T. Uppal, X. Hu, F. R. Fronczek, S. Maschek, P. Bobadova-Parvanova and M. G. H. Vicente, *Chem. Eur. J.*, 2012, **18**, 3893–3905.
- 23 V. Leen, T. Leemans, N. Boens and W. Dehaen, *Eur. J. Org. Chem.*, 2011, 4386–4396.
- 24 C. Yu, Y. Xu, L. Jiao, J. Zhou, Z. Wang and E. Hao, *Chem. Eur. J.*, 2012, **18**, 6437–6442.
- 25 J. C. Phillips, R. Braun, W. Wang, J. Gumbart, E. Tajkhorshid, E. Villa, C. Chipot, R. Skeel, L. Kalé and K. Schulten, *J. Comput. Chem.*, 2005, **26**, 1781–1802.
- 26 <https://www.paramchem.org>.
- 27 K. Vanommeslaeghe, E. Hatcher, C. Acharya, S. Kundu, S. Zhong, J. Shim, E. Darian, O. Guvench, P. Lopes, I. Vorobyov *et al.*, *J. Comput. Chem.*, 2010, **31**, 671–690.
- 28 K. Song, P. Livanec, J. Klauda, K. Kuczera, R. Dunn and W. Im, *J. Phys. Chem. B*, 2011, **115**, 6157.
- 29 C. M. Breneman and K. B. Wiberg, *J. Comput. Chem.*, 1990, **11**, 361–373.
- 30 S. Rihn, M. Erdem, A. D. Nicola, P. Retailleau and R. Ziessel, *Org. Lett.*, 2011, **13**, 1916–1919.
- 31 E. Deniz, G. C. Isbasar, O. A. Bozdemir, L. T. Yildirim, A. Siemiarzuck and E. U. Akkaya, *Org. Lett.*, 2008, **10**, 3401–3403.
- 32 Y. Hayashi, S. Yamaguchi, W. Y. Cha, D. Kim and H. Shinokubo, *Org. Lett.*, 2011, **13**, 2992–2995.